2015 International Symposium on Nonlinear Theory and its Applications
NOLTA2015, Kowloon, Hong Kong, China, December 1-4, 2015

A Chaotic Modulation Interface Circuit for Suppressing EMI in Commercial Power Supplies

Junying Niu‡§, Zhong Li§, Yuhong Song‡§, Gary G. Feng♮ and Wolfgang A. Halang§

‡Department of Electronic and Information Engineering, Shunde Polytechnic, 528300 GuangZhou, P. R. China
§Faculty of Mathematics and Computer Science, FernUniversität in Hagen, 58084 Hagen, Germany
♮ College of Science and Engineering, City University of Hong Kong, Hong Kong, China
Email: niujunying@foxmail.com, Zhong.Li@fernuni-hagen.de, Syhscut@163.com,
megfeng@cityu.edu.hk, Wolfgang.Halang@fernuni-hagen.de

Abstract—To reduce electromagnetic interference(EMI) in commercial switching mode power supplies(SMPS) by chaotic carrier-frequency modulation(CCFM) technique, an interface module based on Chua's circuit is designed to modulate the oscillator frequency of typical pulsewidth-modulated(PWM) IC. With the various component value in Chua's circuit, the switching period modulated by the module obeys different probability distributions. Further, by formulating the power spectral density(PSD) of the chaotic switching PWM sequence, it is found that the effectiveness on EMI reduction depends on the probability density function(PDF) and the randomness level of the switching period. Theoretical predictions are verified with simulations.

1. Introduction

The frequency modulation technique is a high-efficiency approach to reduce EMI of SMPS. By dithering the switching frequency around the nominal value, the discrete harmonic power that usually exists in classical PWM scheme can be spread over a wider frequency range. Periodic signal, randomized signal and chaotic signal have been applied to modulate the switching frequency. By comparison[1–3], the randomized modulation and the chaotic modulation are not only more effective to restrain EMI than periodic modulation, but also more flexible with the variable random degree, due to that the effectiveness on EMI suppression depends on the statistical character of the modulation signal. However, it is difficult to obtain the real random signal, especially the analogue random signal. On the contrary, the chaotic signal is easier to be generated in both the analogue way[4–6] and digital way[7]. Hence, chaotic modulation has attracted an increasing interest of researchers in the recent two decades.

So far, most of the works on CCFM adopt the idealized and simplified models for theoretical study, and CCFM has not been applied in the commercial products yet. Practically, a control IC with an internal carrier and its peripheral circuit are used to form the control circuit, instead of traditionally using separate components.

In this paper, a CCFM interface circuit with features of low cost, simplicity, flexibility and universality is designed for the frequency programmable PWM IC. Further more, by formulating the PSD of the switching pulse under chaos control, it is found that the spread-spectrum effect is related with the randomness level and the PDF of the switching period. In [2, 8], the switching period modulated by Chua's circuit is approximatively considered as following the triangular distribution. However, according to the statistical result, the switching period obeys different distributions with the various component value in Chua's circuit. The spectrum of chaotic PWM pulse are analyzed and compared, while the switching period follows the uniform, the triangle and the inverted triangle distribution. As a result, the best effect of EMI suppression is obtained as the switching period is uniform distribution.

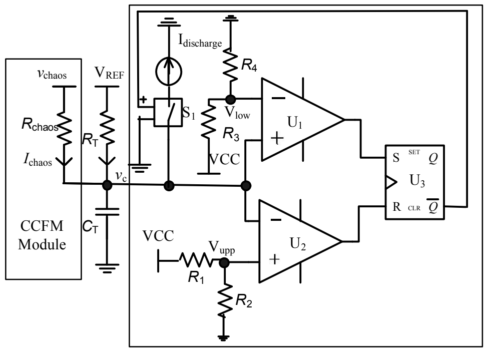

Figure 1: The diagram of PWM IC 's oscillator

2. Design of the CCFM Module

As show in Fig.1, the oscillator of frequency programmable PWM IC's makes use of a timing capacitor and a timing resistor(or only a timing capacitor) to set the switching frequency. The timing capacitor C_T is charged and discharged circularly between V_{low} and V_{upp}, and the switching period is the summation of the charging and discharging time. As a chaotic charging current generated by the CCFM module is supplied to C_T, the switching frequency is dithered chaotically.

The CCFM module, which is shown in Fig.2, is com-

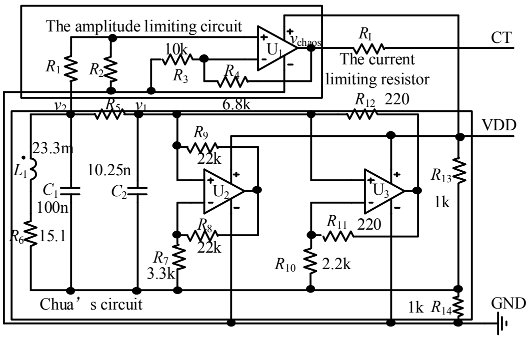

Figure 2: The schematic of the CCFM module

posed of Chua's circuit, an amplitude limiting circuit, and a current limiting resistor. By the amplitude limiting circuit, the chaotic voltage v_2, generated by Chua's circuit, is set to v_{chaos} within a certain range, and v_{chaos} can be calculated as

$$v_{\text{chaos}} = \frac{(R_3 + R_4)R_2 v_2}{(R_1 + R_2)R_3}. \tag{1}$$

Through the current limiting resistor, the chaotic charging current I_{chaos} is supplied to C_{T}. Hence, during the kth switching cycle, the charging time is

$$t_{c_k}(v_{\text{chaos}}, R_{\text{I}}) = \frac{R_{\text{T}} R_{\text{I}}}{R_{\text{T}} + R_{\text{I}}} C_{\text{T}} \ln \frac{\text{V}_{\text{low}} - \frac{R_{\text{I}}\text{V}_{\text{REF}} + R_{\text{T}} v_{\text{chaos}}}{R_{\text{T}} + R_{\text{I}}}}{\text{V}_{\text{upp}} - \frac{R_{\text{I}}\text{V}_{\text{REF}} + R_{\text{T}} v_{\text{chaos}}}{R_{\text{T}} + R_{\text{I}}}}. \tag{2}$$

As the discharging current $\text{I}_{\text{discharge}}$ is far larger than the charging current, the discharging time is approximately 0. Then the frequency of the oscillator is

$$f(v_{\text{chaos}}, R_{\text{I}}) = \frac{1}{t_{c_k}(v_{\text{chaos}}, R_{\text{I}})} = \text{F} + \Delta f(\Delta f \in [0, \Delta F]), \tag{3}$$

where F is the minimum of the frequency as v_{chaos} is minimized to v_{min}. $\triangle F$ is the varied range of the frequency, and can be calculated by $\triangle F = f(v_{\text{max}}, R_{\text{I}}) - f(v_{\text{min}}, R_{\text{I}})$, where v_{max} is the maximum of v_{chaos}. It is apparent that the frequency range can be set easily by adjusting R_{I}, as the parameters of the amplitude limiting circuit are fixed.

3. The Statistical Property of the Switching Period

In [2, 9, 10], Chua's circuit is used to generate the chaotic period, which is regarded as following triangular distribution. However, it is observed that the switching period obeys different distributions with various R_5(see Fig.2). Fig.3 describes the statistical property of the kth switching period T_k with different value of R_5, which determines the state of Chua's circuit. In this paper, T_k is treated as following the uniform, the triangle and the inverted triangle distribution, and the PDF's are expressed as follows:

$$p_1(T_k) = \begin{cases} \left|\dfrac{4(T_k - E[T_k])}{\Re^2}\right|, & T_k \in [E[T_k] - \frac{\Re}{2}, E[T_k] + \frac{\Re}{2}] \\ 0, & \text{else} \end{cases}, \tag{4}$$

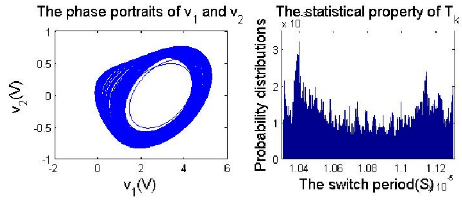

(a) $R_5 = 1.988k\Omega$

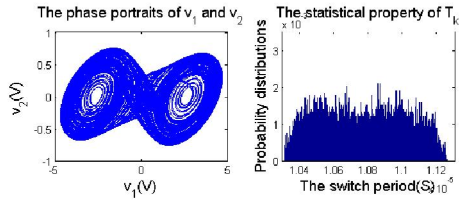

(b) $R_5 = 1.95k$

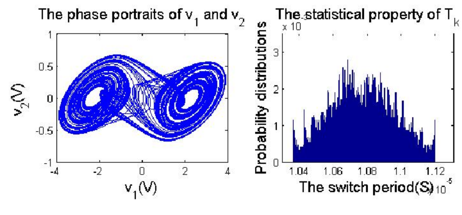

(c) $R_5 = 1.80k$

Figure 3: The statistical property of the switching period

$$p_2(T_k) = \begin{cases} \dfrac{1}{\Re E[T_k]}, & T_k \in [E[T_k] - \frac{\Re}{2}, E[T_k] + \frac{\Re}{2}] \\ 0, & \text{else} \end{cases}, \tag{5}$$

$$p_3(T_k) = \begin{cases} \left|\dfrac{4(T_k - E[T_k] + \frac{\Re}{2})}{\Re^2}\right|, & T_k \in [E[T_k] - \frac{\Re}{2}, E[T_k] + \frac{\Re}{2}] \\ 0, & \text{else} \end{cases}, \tag{6}$$

where $E[\cdot]$ is the expectation operator, and $E[T_k] = \frac{T_{max} + T_{min}}{2}$. For studying the relationship between the randomness degree and the performance of EMI reduction, the amplitude variation level $\Re$ is defined as

$$\Re = \frac{T_{\text{max}} - T_{\text{min}}}{E[T_k]}. \tag{7}$$

According to (3), $\Re$ can be expressed as

$$\begin{aligned} \Re &= 2\frac{T_k(v_{\text{min}}, R_{\text{I}}) - T_k(v_{\text{max}}, R_{\text{I}})}{T_k(v_{\text{min}}, R_{\text{I}}) + T_k(v_{\text{max}}, R_{\text{I}})} \\ &= 2\frac{\ln\frac{[(R_{\text{T}}+R_{\text{I}})\text{V}_{\text{low}} - R_{\text{I}}v_{REF} + R_{\text{T}}v_{\text{min}}][(R_{\text{T}}+R_{\text{I}})\text{V}_{\text{upp}} - R_{\text{I}}\text{V}_{\text{REF}} + R_{\text{T}}v_{\text{max}}]}{[(R_{\text{T}}+R_{\text{I}})\text{V}_{\text{low}} - R_{\text{I}}\text{V}_{\text{REF}} + R_{\text{T}}V_{\text{max}}][(R_{\text{T}}+R_{\text{I}})\text{V}_{\text{upp}} - R_{\text{I}}\text{V}_{\text{REF}} + R_{\text{T}}v_{\text{min}}]}}{\ln\frac{[(R_{\text{T}}+R_{I})\text{V}_{\text{low}} - R_{\text{I}}\text{V}_{\text{REF}} + R_{\text{T}}v_{min}][(R_{\text{T}}+R_{\text{I}})v_{\text{low}} - R_{\text{I}}\text{V}_{\text{REF}} + R_{\text{T}}v_{max}]}{[(R_{\text{T}}+R_{\text{I}})\text{V}_{\text{upp}} - R_{\text{I}}\text{V}_{\text{REF}} + R_{\text{T}}v_{\text{max}}][(R_{\text{T}}+R_{\text{I}})\text{V}_{\text{upp}} - R_{\text{I}}\text{V}_{\text{REF}} + R_{\text{T}}v_{\text{min}}]}} \end{aligned}. \tag{8}$$

Thus, the randomness degree of T_k is determined by R_{I}.

4. The Spectrum of PWM Switching Pulse

Fig.4 shows the waveform of a switching PWM pulse $g(t)$. $g(t)$ has two discrete levels, which is 1 as the switch is on, and 0 as the switch is off. The switching waveform of the kth switching cycle $g_k(t - t_k)$ can be expressed as

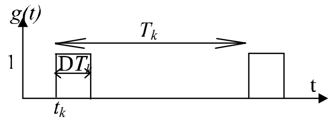

Figure 4: Waveform of a switching PWM pulse train

$$g_k(t-t_k) = \begin{cases} 1, & t_k \leqslant t \leqslant \mathrm{D}T_k + t_k \\ 0, & \text{else} \end{cases}, \quad (9)$$

where D is the duty cycle, $\mathrm{D}T_k$ is the duty time, and t_k is the starting time of the kth switching period.

A general expression for $g(t)$ is

$$g(t) = \lim_{N\to\infty} \sum_{k=1}^{N} g_k(t-t_k). \quad (10)$$

The autocorrelation of $g(t)$[2] is defined as

$$R_g(\tau) = E\left[\lim_{T\to\infty} \frac{1}{T}\int_0^T g(t)g(t+\tau)dt\right]. \quad (11)$$

By using Wiener-Khintchine theorem, the PSD of $g(t)$ is the Fourier transform of its autocorrelation, so it can be expressed by

$$S_g(f) = \int_{-\infty}^{\infty} R_g(\tau)e^{-j2\pi f\tau}d\tau. \quad (12)$$

Following the methodology in [2], (12) is equal to

$$S_g(f) = \frac{1}{E[T_k]}\left\{E\left[|G(f)|^2\right] + 2Re\left(\frac{E\left[G(f)e^{j2\pi fT_k}\right]E\left[G^*(f)\right]}{1-E\left[e^{j2\pi fT_k}\right]}\right)\right\}, \quad (13)$$

where $G(f)$ is defined as

$$G(f) = \frac{2 - \int_{E[T_k]-\frac{E[T_k]\Re}{2}}^{E[T_k]+\frac{E[T_k]\Re}{2}} (p(T_k)e^{-j2\pi f\mathrm{D}T_k} - p(T_k)e^{j2\pi f\mathrm{D}T_k})dT_k}{(2\pi f)^2}. \quad (14)$$

Thus,

$$E\left[|G(f)|^2\right] = \int_{T_{min}}^{T_{max}} p(T_k)G(f)G^*(f)dT_k, \quad (15)$$

$$E\left[G(f)e^{j2\pi fT_k}\right] = \frac{j}{2\pi f}\left(\int_{E[T_k]-\frac{E[T_k]\Re}{2}}^{E[T_k]+\frac{E[T_k]\Re}{2}} p(T_k)e^{j2\pi fT_k(1-\mathrm{D})}dT_k - P(f)\right), \quad (16)$$

$$E[G^*(f)] = 1 - \frac{1}{2\pi f}\int_{E[T_k]-\frac{E[T_k]\Re}{2}}^{E[T_k]+\frac{E[T_k]\Re}{2}} p(T_k)e^{j2\pi f\mathrm{D}T_k}dT_k, \quad (17)$$

$$E\left[e^{j2\pi fT_k}\right] = \int_{E[T_k]-\frac{E[T_k]\Re}{2}}^{E[T_k]+\frac{E[T_k]\Re}{2}} p(T_k)e^{j2\pi fT_k}dT_k. \quad (18)$$

For simplifying calculation, it is assumed that $\mathrm{D}E[T_k]$ is constant and $E[T_k] = 1$, and then $S_g(f)$[11] can be rewritten as follows:

$$S_g(f) = \mathrm{D}^2 Sa^2(\pi f\mathrm{D})\left[1 + 2Re\left(\frac{P(f)}{1-P(f)}\right)\right], \quad (19)$$

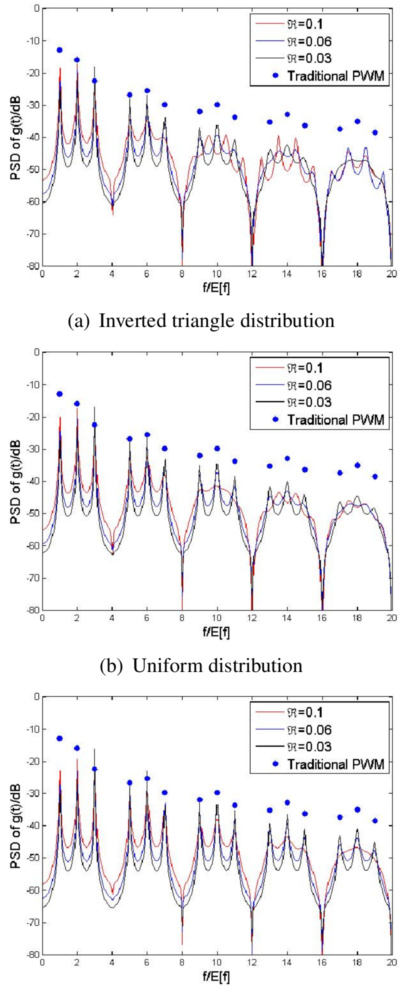

(a) Inverted triangle distribution

(b) Uniform distribution

(c) Triangle distribution

Figure 5: PSD of PWM pulse train with chaotic frequency

where $P(f) = \int_{1-\frac{\Re}{2}}^{1+\frac{\Re}{2}} p(T_k)e^{j2\pi fT_k}dT_k$.

It is remarked that $S_g(f)$ is determined by $P(f)$, which is related to the PDF and the randomness degree of the switching period. Fig.5 shows the calculated PSD's of $g(t)$, as T_k obeys different distributions and with various randomness degree. Under traditional PWM, there are peaks(the blue point) on the switching frequency and its multiplications, resulting in a discrete spectrum. Those peaks are reduced and spread over a frequency band within a certain range under CCFM, and the spectrum becomes continue. The best effect on EMI suppression is obtained as T_k is uniform distribution. The general result is worst while T_k is triangle distribution. The amplitude of spectrum reduction is larger and larger as the randomness increases. Nevertheless, considering that the ripple of the output voltage will increase with a larger randomness level, $/Re$ should be limited by the output requirement, rather than as large as possible.

5. Simulations

A flyback converter controlled by UC3842 is used as example. The spectrums of the primary winding current are given by Fig.6, Fig.7 and Fig.8. To make a comparison, the spectrum under traditional PWM is drawn in red, and the spectrum under CCFM PWM in green. The simulation results accord with the theoretical analysis.

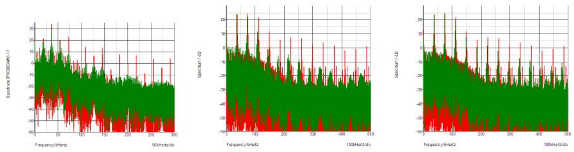

(a) $\Re = 0.1$ (b) $\Re = 0.06$ (c) $\Re = 0.03$

Figure 6: EMI reduction as T_k is inverter triangle distribution

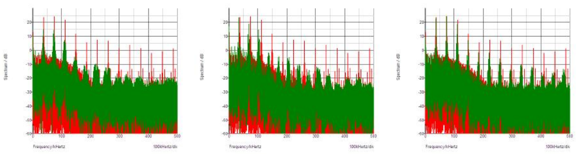

(a) $\Re = 0.1$ (b) $\Re = 0.06$ (c) $\Re = 0.03$

Figure 7: EMI reduction as T_k is uniform distribution

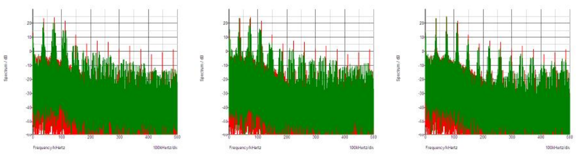

(a) $\Re = 0.1$ (b) $\Re = 0.06$ (c) $\Re = 0.03$

Figure 8: EMI reduction as T_k is triangle distribution

6. Conclusion

Chua's circut is used to design an interface module to carry out CCFM on commercial SMPS's. The switching period of converter can be regarded as a random variable with different PDF. The spectrum characteristic of the switching pulse is formulated, and it is related to the PDF and the randomness of the switching period. The calculated results and simulation results shows that a superior effectiveness of EMI reduction is obtained by increasing the randomness and using the uniform distribution.

Acknowledgement

This work was supported by AvH-Institutspartnerschaft under grant No. 2.4-IP-DEU/1009882.

References

[1] K. Tse, H.-H. Chung, S. R. Hui, and H. So, "A comparative study of carrier-frequency modulation techniques for conducted EMI suppression in PWM converters," *Industrial Electronics, IEEE Transactions on*, vol. 49, no. 3, pp. 618–627, 2002.

[2] K. Tse, R.-M. Ng, H.-H. Chung, and S. R. Hui, "An evaluation of the spectral characteristics of switching converters with chaotic carrier-frequency modulation," *Industrial Electronics, IEEE Transactions on*, vol. 50, no. 1, pp. 171–182, 2003.

[3] J. Jankovskis, D. Stepins, S. Tjukovs, and D. Pikulins, "Examination of different spread spectrum techniques for EMI suppression in dc/dc converters," *Electronics and Electrical Engineering.–Kaunas: Technologija*, no. 6, p. 86, 2008.

[4] L. O. Chua, L. Kocarev, K. Eckert, and M. Itoh, "Experimental chaos synchronization in Chua's circuit," *International Journal of Bifurcation and Chaos*, vol. 2, no. 03, pp. 705–708, 1992.

[5] K. M. Cuomo, A. V. Oppenheim, and S. H. Strogatz, "Synchronization of Lorenz-based chaotic circuits with applications to communications," *Circuits and systems II Analog and digital signal processing, IEEE Transactions on*, vol. 40, no. 10, pp. 626–633, 1993.

[6] G. Zhong and W. K. Tang, "Circuitry implementation and synchronization of Chen's attractor," *International Journal of Bifurcation and Chaos*, vol. 12, no. 06, pp. 1423–1427, 2002.

[7] R. M. May *et al.*, "Simple mathematical models with very complicated dynamics," *Nature*, vol. 261, no. 5560, pp. 459–467, 1976.

[8] Z. Li, S. Qiu, and Y. Chen, "Experimental study on the suppressing EMI level of DC-DC converter with chaotic map," *Proceedings of the CSEE*, vol. 5, p. 012, 2006.

[9] G. Li, X. Chen, and F. Liu, "Analysis of power spectral density of the output voltage in chaotic PWM inverter," *Proceedings of the Chinese Society of Electrical Engineering*, vol. 26, no. 20, pp. 79–83, 2006.

[10] W. Zhou and S. Qiu, "Effect of chaotic spectrum-spread on output voltage ripple of power converter," *Electric Power Automation Equipment*, vol. 12, p. 014, 2008.

[11] T. TANAKA, H. KAMEDA, and T. NINOMIYA, "Noise analysis of DC-to-DC converter with random-switching control," *IEICE TRANSACTIONS on Communications*, vol. 75, no. 11, pp. 1142–1150, 1992.